Published in final edited form as:
Nucl Med Biol. 2010 April ; 37(3): 365–370. doi:10.1016/j.nucmedbio.2009.12.005.

Biodistribution and Stability Studies of [^{18}F]Fluoroethylrhodamine B, a Potential PET Myocardial Perfusion Agent

Vijay Gottumukkala[1,2], **Tobias K. Heinrich**[1,2,*], **Amanda Baker**[1], **Patricia Dunning**[1], **Frederick H Fahey**[1,2], **S. Ted Treves**[1,2], and **Alan B. Packard**[1,2,†]

[1] Division of Nuclear Medicine, Department of Radiology, Children's Hospital Boston

[2] Harvard Medical School, Boston, Massachusetts

Abstract

Introduction—Fluorine-18-labeled rhodamine B was developed as a potential PET tracer for the evaluation of myocardial perfusion, but preliminary studies in mice showed no accumulation in the heart suggesting that it was rapidly hydrolyzed *in vivo* in mice. A study was, therefore, undertaken to further evaluate this hypothesis.

Methods—[^{18}F]Fluoroethylrhodamine B was equilibrated for 2 h at 37 °C in human, rat and mouse serum and in PBS. Samples were removed periodically and assayed by HPLC. Based on the results of the stability study, microPET imaging and a biodistribution study were carried out in rats.

Results—*In vitro* stability studies demonstrated that [^{18}F]fluoroethylrhodamine B much more stable in rat and human sera than in mouse serum. After 2 h, the compound was >80% intact in rat serum but <30% intact in mouse serum. The microPET imaging and biodistribution studies in rats confirmed this result showing high and persistent tracer accumulation in the myocardium compared with the absence of uptake by the myocardium in mice thereby validating our original hypothesis that ^{18}F-labeled rhodamines should accumulate in the heart.

Conclusions—[^{18}F]Fluoroethyl rhodamine B is more stable in rat and human sera than it is in mouse serum. This improved stability is demonstrated by the high uptake of the tracer in the rat heart in comparison to the absence of visible uptake in the mouse heart. These observations suggest that ^{18}F-labeled rhodamines are promising candidates for more extensive evaluation as PET tracers for the evaluation of myocardial perfusion.

Keywords

rhodamine B; fluorine-18; myocardial perfusion imaging; positron emission tomography

1. Introduction

There are currently several PET tracers available for myocardial perfusion imaging (MPI) including [^{15}O]H_2O, [^{13}N]NH_3, and ^{82}Rb. However, the short half-lives of ^{15}O (2 min.) and ^{13}N (10 min.) limit their availability to those institutions with on-site cyclotrons.

†Correspondence author at: Division of Nuclear Medicine, Children's Hospital, 300 Longwood Ave., Boston, MA 02115. Phone: 001-617-355-7539 Fax: 001-617-730-0619 alan.packard@childrens.harvard.edu.
*Current address: Molecular Imaging Research, Bayer Schering Pharma AG, Muellerstrasse 178, 13353 Berlin, Germany

Rubidium-82 ($t_{1/2}$ = 76 s) is more widely available because it is produced by the $^{82}Sr/^{82}Rb$ generator, but high patient throughput is required to offset the high cost of the generator. These limitations have spurred interest in the development of an ^{18}F-labeled MPI radiopharmaceutical [1,2]. Fluorine-18 offers the advantages of high positron yield of ^{18}F (97%), its half-life (110 min.) allows repeated studies within the same day, and the distribution networks that have been established for [^{18}F]FDG have demonstrated that production of ^{18}F-labeled radiopharmaceuticals at central sites is a reasonable alternative to on-site production.

A number of ^{18}F compounds have been proposed as possible myocardial perfusion agents including quaternary ammonium salts [3], tetraphenylphosphonium compounds [4–8] rotenone [9], and BMS-747158-02, a pyridazinone analog [10]. Of these, the most promising is perhaps BMS-747158-02, which was optimized to target mitochondrial complex I [11,12] and shows better correlation between extraction and flow than the single-photon tracers ^{99m}Tc-MIBI and ^{201}Tl or the PET tracer [^{13}N]NH_3 [12]. One possible limitation to this compound may be *in vivo* defluorination, although this is apparently lower in non-human primates than in rodents [13].

We recently reported the synthesis of ^{18}F-labeled rhodamine B (Fig. 1) as potential myocardial perfusion agent [14–17]. The compound is a lipophilic cation as are the single-photon myocardial perfusion agents ^{99m}Tc-MIBI and ^{99m}Tc-tetrofosmin and several of the ^{18}F-labeled compounds listed above. Non-radiolabeled rhodamines are known to accumulate in the mitochondria in proportion to mitochondrial membrane potential [18–21] and are substrates for Pgp, a protein implicated in multidrug resistance [22,23]. Vora and Dhalla previously reported that non-radiolabeled rhodamine 123 accumulated in the mouse heart [24]. However, in our previous studies of 2′-[^{18}F]fluoroethylrhodamine B we observed no accumulation of the tracer in the mouse heart and suggested that this may be due to *in vivo* hydrolysis of the 2-fluoroethylester [16]. In the present work, we further examine this hypothesis by measuring the stability of 2′-[^{18}F]fluoroethylrhodamine B in various sera. Based on the results of these *in vitro* studies, we evaluated the biodistribution of 2′-[^{18}F]fluoroethylrhodamine B in a rat and found significant and persistent uptake in the myocardium.

2. Materials and methods

2.1. General

Rhodamine B lactone (>97%) was purchased from MP Biomedicals (Solon, OH). Ethylene glycol ditosylate (>97%) was purchased from Sigma-Aldrich (St. Louis, MO). Extra dry reagent grade acetonitrile and Kryptofix® (K2.2.2) (98%) were purchased from Fluka (St. Louis, MO). Potasssium carbonate (99.997%) was purchased from Alfa Aesar (Ward Hill, MA). Human, rat and mouse sera were purchased from Sigma-Aldrich (St. Louis, MO). Other solvents and reagents were of the highest grade commercially available and were used as received unless otherwise noted. Thin-layer chromatography (TLC) was performed using Silicagel IB-F coated plastic sheets from J.T. Baker (Phillipsburg, NJ). ^{1}H-Nuclear magnetic resonance (NMR) spectra were obtained using a Varian 400 spectrometer (Palo Alto, CA). Mass spectra were obtained using a Thermo-Finnigan LTQ Mass Spectrometer (ESI-MS mode) through the courtesy of Prof. Elena V. Rybak-Akimova (Tufts University). Fluorine-18 (in water) was purchased from Cardinal Healthcare (Woburn, MA).

2.2 Purification and quality control

Analytical high-performance liquid chromatography (HPLC) was carried out using an HITACHI 7000 system including an L-7455 diode array detector, an L-7100 pump, and a D-7000 interface. The radiometric HPLC detector was comprised of Canberra nuclear instrumentation modules and optimized for 511 keV photons. An LaChrom PuroSphere Star

C18e column (4 × 30 mm, 3 μm) was used for analytical measurements. The solvent system was 0.1% trifluoroacetic acid (TFA) in water (solvent A) and 0.1% TFA in acetonitrile (solvent B) at a flow rate of 1 mL/min at room temperature. The solvent gradient was 0–15 min (30%–70% B), 15–25 min. (70% B). The serum stability graph was created from the raw HPLC data using GraphPad Prism (GraphPad Software, Inc., La Jolla, CA 92037 USA).

For semi-preparative HPLC, an ISCO system comprised of an ISCO V^4 variable wavelength UV-visible detector (operated at λ=550 nm), an ISCO 2300 HPLC pump, a Canberra gamma detector, and a Grace Apollo C18 column (10 × 250 mm, 5μm) was used. Semi-preparative HPLC method (isocratic): 40% 0.1% trifluoroacetic acid (TFA) in water; 60% 0.1% TFA in acetonitrile; flow rate – 5 mL/min.; room temperature.

Radiofluorination yields were determined by thin-layer chromatography using silica gel plates and chloroform:methanol (8:1 v/v) as the solvent. After they were developed, the TLC strips were cut into 1 cm pieces and counted with a Packard Cobra gamma counter.

2.3. Preparation of [^{18}F]FERhB (1)

2′-[^{18}F]fluoroethylrhodamine B ([^{18}F]FERhB) was prepared as described previously [16] and characterized by HPLC and TLC using the non-radiolabeled (^{19}F) compound as a reference except that in this work the [^{18}F]fluoroethyl tosylate precursor was purified by semi-preparative HPLC prior to synthesis of the 2′-[^{18}F]fluoroethylester. The [^{18}F]fluoroethyl tosylate reaction mixture was cooled and dissolved in 0.5 mL acetonitrile and 0.2 mL water, filtered, and injected into the HPLC (conditions as above). Purified [^{18}F]fluoroethyl tosylate was collected, diluted 10X with water and passed through a C18 SepPak cartridge (Waters). The SepPak cartridge was dried a stream of nitrogen, and the product was eluted into a reaction vial with 1.5 mL of acetonitrile.

The [^{18}F]FERhB was then synthesized and purified as previously described using the purified precursor.

2.4. Serum stability study

The serum stability study was carried out using a procedure similar to that described by Kronauge, et al. [25]. HPLC-purified [^{18}F]FERhB was dried under a stream of nitrogen and dissolved in 10% ethanol/PBS. For each experiment, to 200 μL of serum in a borosilicate culture tube equilibrated to 37°C in a water bath was added 1.5–3.7 MBq (40–100 μCi) of [^{18}F]FERhB in 20 μL 10% ethanol/PBS. The tubes were shaken and the samples were placed back in the water bath. At selected time points (15, 30, 60 and 120 min.) enzymatic hydrolysis was stopped with the addition of cold (4°C) absolute ethanol (1 mL), the samples were cooled in an ice bath to precipitate serum proteins, centrifuged (15 mm, 2500 x g, 4°C), and the supernatant was analyzed by HPLC. The percentage intact [^{18}F]FERhB at each time point was calculated from the chromatograms.

2.5. Animal studies

Animal studies were carried out under a protocol approved by the Children's Hospital Boston Institutional Animal Care and Use Committee. The HPLC-purified compound was evaporated to dryness (to remove acetonitrile and trifluoractic acid) and dissolved in 10% ethanol in saline for injection. Animals were injected with 100 μL (3.7–5.6 MBq, 100–150 μCi) of [^{18}F]FERhB. Immediately after injection the animals were anesthetized with isofluorane (2–4% in air) and image acquisition initiated as quickly as possible. Imaging was performed using a Siemens Focus 120 MicroPET scanner. Data were acquired for 60 min. in list mode and reconstructed either into a single 60 min. image or 12 300-s frames. Reconstruction was performed using unweighted OSEM2D generating an image with a volume of 128 × 128 × 95 voxels (0.866 ×

$0.866 \times 0.796\ mm^3$). The ASIPro software package (Siemens Medical Solutions) was used for image analysis. Time-activity curves were constructed by manually drawing regions of interest (ROI) within the left ventricular myocardium and medially in the liver, closer to the diaphragmatic border on a coronal slice in the first frame. This ROI was then copied on each of the frames, and the mean activities within the ROIs were plotted as time-activity curves (TACs).

2.6. Biodistribution study

The biodistribution of [^{18}F]FERhB was measured in four Fischer rats (male, 150 g) with jugular vein catheters. Each animal was injected via the catheter with 0.5–1.3 MBq (15–35 μCi) of [^{18}F]FERhB in 100 μL 10% EtOH/saline. At 1 h post–injection, the animals were sacrificed by CO_2 euthanasia, and selected tissues excised, weighed, and assayed for ^{18}F. The percent injected dose per gram (% i.d./g) for each tissue was calculated by comparison of the tissue counts to a standard sample prepared from the injectate.

3. Results and discussion

3.1. Synthesis of ^{18}F-labeled rhodamine B

The radiosynthesis of [^{18}F]FERhB was accomplished using the previously described one-pot synthesis [16]. This produced the desired product in a decay-corrected yield of 35% and 97% radiochemical purity. The specific activity was 2.5 GBq/μmol, and the total synthesis time was approximately 90 min. The apparent specific activity of the product is higher than that previously reported because the purification of the [^{18}F]fluoroethyl tosylate to remove unreacted 1,2-ditosylethane reduced contamination of the final product with by-products formed by the reaction of 1,2-ditosylethane with rhodamine B lactone. These by-products (i.e., 2′-tosylethylrhodamine B and 2′-hydroxyethylrhodamine, formed by in situ hydrolysis of 2′-tosylethylrhodamine B) are not separated from [^{18}F]FERhB in the final semi-preparative HPLC purification because they are chemically very similar, the only difference being a terminal -F versus -OH (or -OTs) on the ethylester.

3.2 Serum stability study

The data summarized in Figure 2 clearly show that [^{18}F]FERhB is rapidly hydrolyzed in mouse serum with 87% present as the intact compound after 15 min. in mouse serum at 37 °C and only 29% remaining after 2 h. In contrast, the compound is 95% intact in human serum after 2 h of incubation at 37 °C and 86% intact in rat serum after 2 h. As expected, there was no decomposition of the control sample in PBS. The stability differences can also be clearly seen in the chromatogram from which Figure 2 was derived (Fig. 3).

The presumed decomposition products of rhodamine B 2′-fluoroethyl ester are the non-radioactive rhodamine B acid and ^{18}F-labeled 2-fluoroethanol. No effort was made to characterize the ^{18}F-labeled decomposition products because it is well known that ethyl esters are susceptible to rapid hydrolysis in mouse serum [25]. The addition of the very electrophilic fluoride atom to the ethyl moiety will further increase this susceptibility, as shown by the large difference between the pK_as of ethanol (15.9) and 2-fluoroethanol (12.4) [26]. The 2-fluoroethanol would itself then be metabolized to the 2-fluoroacetic acid [27]. In this context, it's interesting to note that, despite the extensive use of the 2-[^{18}F]fluoroethyl moiety in PET chemistry, the biodistribution of 2-[^{18}F]fluoroethanol has apparently not been reported [28]. In the absence of these data, one can only speculate about whether or not the gall bladder excretion that was observed for [^{18}F]FERh in the mouse is consistent with the production of 2-[^{18}F]fluoroethanol and its metabolites.

The observed decomposition of the ester in mouse serum parallels the observations of Harapanhalli, et al. who reported that approximately 10% of the iodinated rhodamine 123 was still present in mouse blood as the ester 2 h post-injection [29]. Vora and Dhalla also reported *in vivo* hydrolysis of non-labeled rhodamine 123 (a methyl ester) to rhodamine 110 (the acid form) in mice, but still noted high rhodamine uptake in the heart, perhaps because the larger physical quantity of the non-labeled material inhibited hydrolysis [24]. However, the much slower rate of decomposition in rat and human serum observed in our *in vitro* study suggested that improved results might be obtained in a different animal model.

3.3. Small-animal PET imaging

In contrast to the absence of myocardial uptake and high uptake in the gall bladder that was observed when [^{18}F]FERhB was injected into mice [16], microPET images of the distribution of [^{18}F]FERhB in rats show significant uptake in the myocardium. The microPET images also reveal high uptake in the liver, gut, spleen, and kidneys (Fig. 4). Also noted is a region of high ^{18}F activity in the region of the neck. The reason for this is unknown at this time, but it is possible that this reflects accumulation in the parathyroid, as is observed with ^{99m}Tc-MIBI [30]. Significant tracer accumulation is also observed in the muscles of the forelimbs, again as is seen with ^{99m}Tc-MIBI. There is minimal uptake in the bone, with the skeleton being barely discernable.

Time-activity curves for the heart and liver were created using data rebinned into 5 min. frames. These curves (Fig. 5) show that tracer concentration in the liver is initially greater than that in the heart but decreases over time such that, at 1 h post-injection, the two concentrations are approximately equal. Throughout this period, the concentration of tracer in the myocardium remains essentially constant, with no appreciable washout. These results are consistent with the hypothesis that the higher stability observed in rat versus mouse serum *in vitro* results in higher myocardial uptake in rats versus mice. This also suggests that equally high uptake might be observed in patients, as the compound is more stable in human serum than it was in rat serum. The advantage of increased uptake by the myocardium is, to some extent, offset by increased uptake by the liver (Fig. 4), which was not seen in the mouse study [16]. It remains to be seen whether other ^{18}F derivatives of this compound can be developed that retain the high myocardial uptake while improving clearance from the liver.

3.4. Biodistribution study

A biodistribution study of [^{18}F]FERhB was carried out in male Fischer rats at 60 min. post-injection to corroborate the results of the microPET imaging study. These results are summarized in Table 1. At 60 min. post-injection, the myocardial uptake is 2.06±0.61% injected dose per gram (%ID/g). This is more than twice the liver concentration (0.89±0.07% ID/g) and more than 25 times the concentration in the blood (0.08±0.03%). There is also significant ^{18}F accumulation in the lungs (1.78±0.65%ID/g), kidney (8.31±0.81%ID/g), gut (2.4±0.53%ID/g), and spleen (5.63±0.78%ID/g). The kidney and gut uptake are consistent with the elimination pattern seen in the microPET images. The high lung and spleen uptake may reflect the tendency of rhodamines to aggregate, even at sub-micromolar concentrations [31]. This possibility is the subject of on-going investigations.

The biodistribution results for [^{18}F]FERhB may be compared to those for BMS-747158-02 [13]. At 30 min. post-injection, the concentration of BMS-747158-02 in the heart is 3.4%ID/g, the liver concentration is 1.3%ID/g, and the blood concentration is 1.2%ID/g. The heart-to-liver ratio is 2.7 and the heart-to-blood ratio is 30. Thus, while the concentration of BMS-747158-02 at 30 min. post-injection in these tissues is higher than that of [^{18}F]FERhB at 60 min, the ratios are quite similar (heart:liver, 2.3 vs. 2.7; heart:blood, 26 vs. 30). At 120 min. post-injection, the concentration of BMS-747158-02 is the heart is essential the same as

it is at 30 min. (3.7%ID/g), while the liver concentration decreases to 0.63%ID/g and the blood concentration increases to 3.41%ID/g. The concentration of [^{18}F]FERhB in the heart also remains essentially constant over 60 min. (Fig. 5) while the liver activity decreases, albeit more slowly than is observed for BMS-747158-02. These investigators also reported evidence of *in vivo* defluorination of BMS-747158-02, which resulted in an increase in tracer uptake in the bone from 1.14±0.13%ID/g at 30 min. post-injection to 2.38±0.28%ID/g at 120 min. post-injection. A similar increase in tracer concentration in the bone was observed in a previous report [12] but was not observed in a third report [10]. In the third study, the tracer concentration in the bone was 0.20±0.01% at 60 min. post-injection, almost an order of magnitude lower than observed in the two previous reports while the only apparent difference from the previous two reports is the use of a different strain of rat for the biodistribution study (Wistar vs. Sprague-Dawley). In contrast, for [^{18}F]FERhB, which is presumably metabolized by ester hydrolysis to produce 2-[^{18}F]fluoroethanol and its metabolites rather than ^{18}F fluoride, the bone uptake (femur) is low (0.45±0.08% ID/g), similar to that observed for BMS-747158-02 in Wistar rats and much lower than observed for BMS-747158-02 in Sprague-Dawley rats.

The ^{18}F-labeled rotenone derivative, ^{18}F-fluorodihydrorotenone ([^{18}F]DHRT), shows high and persistent myocardial uptake with 3.84±0.37%ID/g at 5 min. and 3.71±0.15%ID/g at 120 min. post-injection [32], similar to that observed for BMS-747158-02 and higher than is observed for [^{18}F]FERhB (2.06±0.61%ID/g). Tracer concentration in the blood and bone are low (0.06±0.02%ID/g and 0.52±0.11%ID/g, respectively, at 120 min. post-injection), but no data is available for the liver. These results are similar to those for [^{18}F]FERhB (0.08±0.03% ID/g and 0.45±0.08%ID/g, respectively, at 60 min. post-injection).

It is more difficult to compare the biodistribution of [^{18}F]FERhB to that of the two ^{18}F-labeled tetraphenyl phosphonium derivatives, fluorobenzyl triphenyl phosphonium (FBnTP) [4–7] and fluorophenyl triphenyl phosphonium (FTPP) [8], as there are apparently no reports of the biodistribution of either compound. The only data available for FTPP gives the heart-to-blood ratio as 80 at 30 min., decreasing to 67 at 60 min., suggesting washout from the heart over this time period [8]. No data is presented for liver accumulation. While there are several reports of biological studies of FBnTP [5–7], the only biodistribution data is from PET images of dogs, which show that tracer concentration in the heart and liver are essentially equal out to 90 min. post-injection [5].

4. Conclusion

Having previously described the synthesis of ^{18}F-ethyl-rhodamine B and observed that the compound was apparently rapidly hydrolyzed *in vivo* in the mouse resulting in high gall bladder uptake and no apparent accumulation in the heart, we carried out an *in vitro* study that confirmed that the compound is rapidly hydrolyzed in mouse serum and also observed that it is significantly more stable in rat (and human) serum. Based on these results, a microPET study was carried out that confirmed the results of the *in vitro* study, showing high and persistent accumulation of the tracer in the myocardium in the rat. We also improved the purity of the final product by purifying the [^{18}F]fluoroethyl tosylate precursor prior to fluorination of rhodamine B. The microPET imaging results confirmed our original hypothesis that [^{18}F] fluoroethyl rhodamine B is a promising candidate for further study as a PET myocardial perfusion agent. Additional studies are now underway to further examine the use of [^{18}F] FERhB as a myocardial perfusion agent and also to determine if, like its non-radiolabeled analog [22], it is a substrate for Pgp and can therefore be used in the evaluation of multidrug resistance.

Acknowledgments

These studies were supported by the Children's Hospital Boston Radiology Foundation and NIH grant #5 R01 CA94338 (ABP).

References

1. Higuchi T, Bengel FM. Cardiovascular nuclear imaging: from perfusion to molecular function. Heart 2008;94:809–16. [PubMed: 18480360]
2. Beller GA, Watson DD. A Welcomed New Myocardial Perfusion Imaging Agent for Positron Emission Tomography. Circulation 2009;119:2299–301. [PubMed: 19414654]
3. Studenov AR, Berridge MS. Synthesis and properties of 18F-labeled potential myocardial blood flow tracers. Nuc Med Biol 2001;28:683–93.
4. Ravert HT, Madar I, Dannals RF. Radiosynthesis of 3-[^{18}F]fluoropropyl and 4-[^{18}F]fluorobenzyl triarylphosphonium ions. J Label Compd Radiopharm 2004;47:469–76.
5. Madar I, Ravert HT, Du Y, Hilton J, Volokh L, Dannals RF, et al. Characterization of Uptake of the New PET Imaging Compound ^{18}F-Fluorobenzyl Triphenyl Phosphonium in Dog Myocardium. J Nucl Med 2006;47:1359–66. [PubMed: 16883017]
6. Madar I, Ravert H, DiPaula A, Du Y, Dannals RF, Becker L. Assessment of Severity of Coronary Artery Stenosis in a Canine Model Using the PET Agent ^{18}F-Fluorobenzyl Triphenyl Phosphonium: Comparison with ^{99m}Tc-Tetrofosmin. J Nucl Med 2007;48:1021–30. [PubMed: 17504876]
7. Madar, I.; Gao, D.; Ravert, H.; Chen, L.; Pomper, M.; Dannals, R., et al. ^{18}F-Fluorobenzyltriphenyl phosphonium PET detects area-specific apoptosis in the aging myocardium. Society of Nuclear Medicine, 54th Annual Meeting; Washington, DC. 2007; p. 166
8. Shoup, TM.; Elmaleh, DR.; Brownell, A-L.; Pitman, JT.; Zhu, A.; Wang, X., et al. Evaluation of (4-[^{18}F]fluorophenyl)triphenylphosphonium ion as a potential myocardial blood flow agent for PET. Society of Nuclear Medicine, 52nd Annual Meeting; Toronto, ON. 2005;
9. Marshall RC, Powers-Risius P, Reutter BW, O'Neil JP, La Belle M, Huesman RH, et al. Kinetic Analysis of ^{18}F-Fluorodihydrorotenone as a Deposited Myocardial Flow Tracer: Comparison to ^{201}Tl. J Nucl Med 2004;45:1950–9. [PubMed: 15534068]
10. Huisman MC, Higuchi T, Reder S, Nekolla SG, Poethko T, Wester H-J, et al. Initial Characterization of an ^{18}F-Labeled Myocardial Perfusion Tracer. J Nucl Med 2008;49:630–6. [PubMed: 18344426]
11. Yalamanchili P, Wexler E, Hayes M, Yu M, Bozek J, Kagan M, et al. Mechanism of uptake and retention of F-18 BMS-747158-02 in cardiomyocytes: A novel PET myocardial imaging agent. J Nucl Cardiol 2007;14:782–8. [PubMed: 18022104]
12. Yu M, Guaraldi MT, Mistry M, Kagan M, McDonald JL, Drew K, et al. BMS-747158-02: a novel PET myocardial perfusion imaging agent. J Nucl Cardiol 2007;14:789–98. [PubMed: 18022105]
13. Purohit A, Radeke H, Azure M, Hanson K, Benetti R, Su F, et al. Synthesis and biological evaluation of pyridazinone analogues as potential cardiac positron emission tomography tracers. J Med Chem 2008;51:2954–70. [PubMed: 18422306]
14. Heinrich, TK.; Treves, ST.; Packard, AB. Development of ^{18}F-labeled rhodamine B derivatives for myocardial perfusion imaging with PET. AMI/SMI Joint Molecular Imaging Conference; Providence, RI. 2007;
15. Heinrich, TK.; Fahey, F.; Dunning, P.; Snay, E.; Treves, ST.; Packard, AB. Synthesis and initial in vivo characterization of ^{18}F-labeled rhodamine B: A potential PET myocardial perfusion agent. Society of Nuclear Medicine, 55th Annual Meeting; New Orleans, LA. 2008; p. 302
16. Heinrich TK, Gottumukkala V, Snay E, Dunning P, Fahey FH, Treves ST, et al. Synthesis of fluorine-18 labeled rhodamine B: A potential PET myocardial perfusion imaging agent. Appl Radiat Isot 2010;68:96–100. [PubMed: 19783150]
17. Gottumukkala V, Heinrich TK, Treves ST, Packard AB. Serum stability studies of F-18-ethyl-rhodamine B. J Label Compd Radiopharm 2009;52(Suppl 1):S110.
18. Lacerda SH, Abraham B, Stringfellow TC, Indig GL. Photophysical, photochemical, and tumor-selectivity properties of bromine derivatives of rhodamine-123. Photochem Photobiol 2005;81:1430–8. [PubMed: 16149863]

19. Reungpatthanaphong P, Dechsupa S, Meesungnoen J, Loetchutinat C, Mankhetkorn S. Rhodamine B as a mitochondrial probe for measurement and monitoring of mitochondrial membrane potential in drug-sensitive and -resistant cells. J Biochem Biophys Methods 2003;57:1–16. [PubMed: 12834959]
20. Hu Y, Moraes CT, Savaraj N, Priebe W, Lampidis TJ. Rho(0) tumor cells: a model for studying whether mitochondria are targets for rhodamine 123, doxorubicin, and other drugs. Biochem Pharmacol 2000;60:1897–905. [PubMed: 11108806]
21. Lampidis TJ, Hasin Y, Weiss MJ, Chen LB. Selective killing of carcinoma cells “in vitro” by lipophilic-cationic compounds: a cellular basis. Biomed Pharmacother 1985;39:220–6. [PubMed: 3936557]
22. Rusiecka I, Skladanowski AC. Induction of the multixenobiotic/multidrug resistance system in various cell lines in response to perfluorinated carboxylic acids. Acta Biochim Pol 2008;55:329–37. [PubMed: 18560606]
23. De Moerloose B, Van de Wiele C, Dhooge C, Philippe J, Speleman F, Benoit Y, et al. Technetium-99m sestamibi imaging in paediatric neuroblastoma and ganglioneuroma and its relation to P-glycoprotein. Eur J Nucl Medicine 1999;26:396–403.
24. Vora MM, Dhalla M. In vivo studies of unlabeled and radioiodinated rhodamine-123. Nuc Med Biol 1992;19:405–10.
25. Kronauge JF, Noska MA, Davison A, Holman BL, Jones AG. Interspecies variation in biodistribution of technetium (2-carbomethoxy- 2-isocyanopropane)6+ J Nucl Med 1992;33:1357–65. [PubMed: 1613578]
26. Smart, BE. Characteristics of C-F Systems. In: Banks, RE.; Smart, BE.; Tatlow, JC., editors. Organofluorine Chemistry: Principles and Commercial Applications. New York: Plenum Press; 1994. p. 68
27. Zoghbi SS, Shetty HU, Ichise M, Fujita M, Imaizumi M, Liow J-S, et al. PET imaging of the dopamine transporter with ^{18}F-FECNT: A polar radiometabolite confounds brain radioligand measurements. J Nucl Med 2006;47:520–7. [PubMed: 16513622]
28. Tewson TJ, Welch MJ. Preparation and preliminary biodistribution of “no carrier added” fluorine1–8 fluoroethanol. J Nucl Med 1980;21:559–64. [PubMed: 6770057]
29. Harapanhalli RS, Roy AM, Adelstein SJ, Kassis AI. [^{125}I/^{127}I/^{131}I]Iodorhodamine: Synthesis, cellular localization, and biodistribution in athymic mice bearing human tumor xenografts and comparison with [^{99m}Tc]hexakis(2-methoxyisobutylisonitrile). J Med Chem 1998;41:2111–7. [PubMed: 9622552]
30. Palestro CJ, Tomas MB, Tronco GG. Radionuclide imaging of the parathyroid glands. Semin Nucl Med 2005;35:266–76. [PubMed: 16150247]
31. López Arbeloa I, Ruiz Ojeda P. Dimeric states of rhodamine B. Chem Phys Lett 1982;87:556–60.
32. Martarello L, Greenamyre JT, Goodman MM. Synthesis and evaluation of a new fluorine-18 labeled rotenoid as a potential PET probe of mitochondrial complex I activity. J Label Compd Radiopharm 1999;42:1039–51.

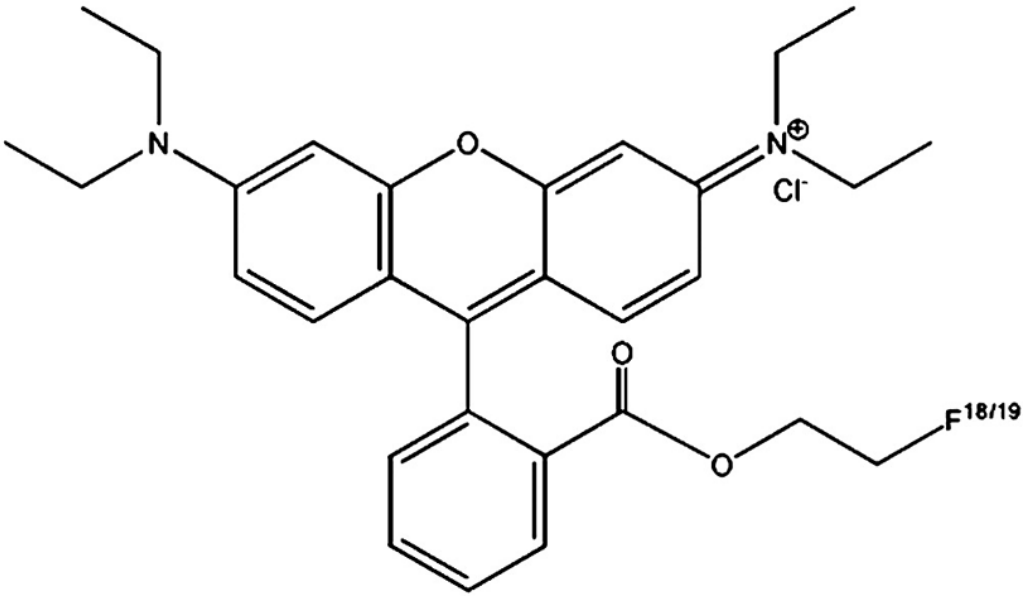

Figure 1.
2′-Fluoroethylrhodamine B

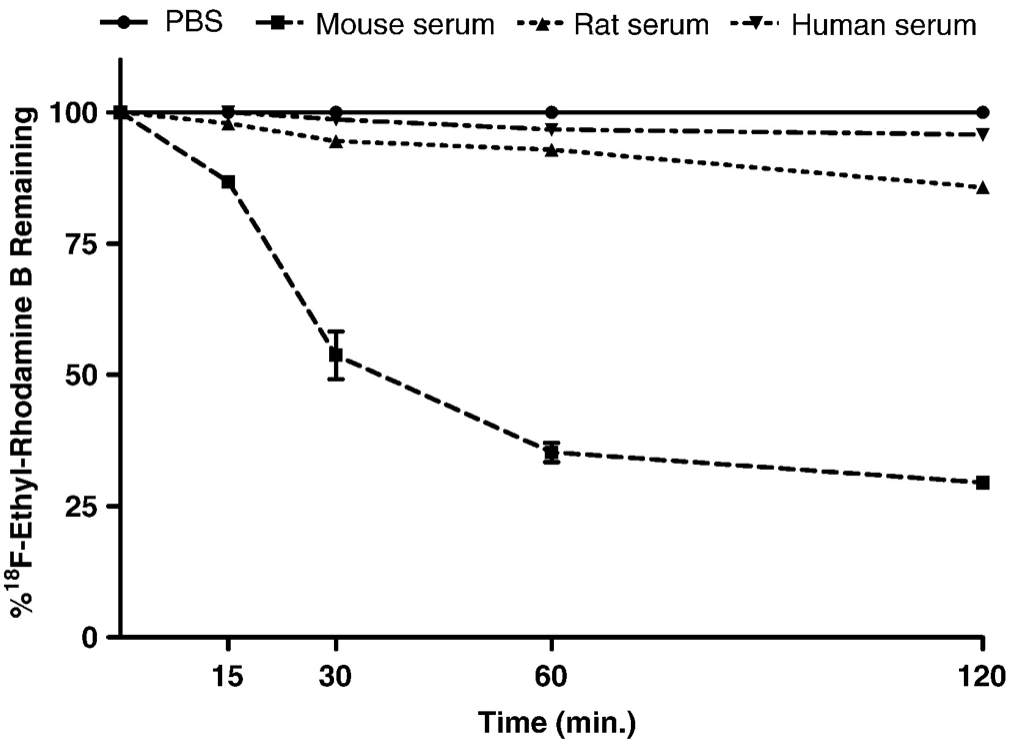

Figure 2.
Stability of 2′-[^{18}F]fluoroethylrhodamine B in various sera

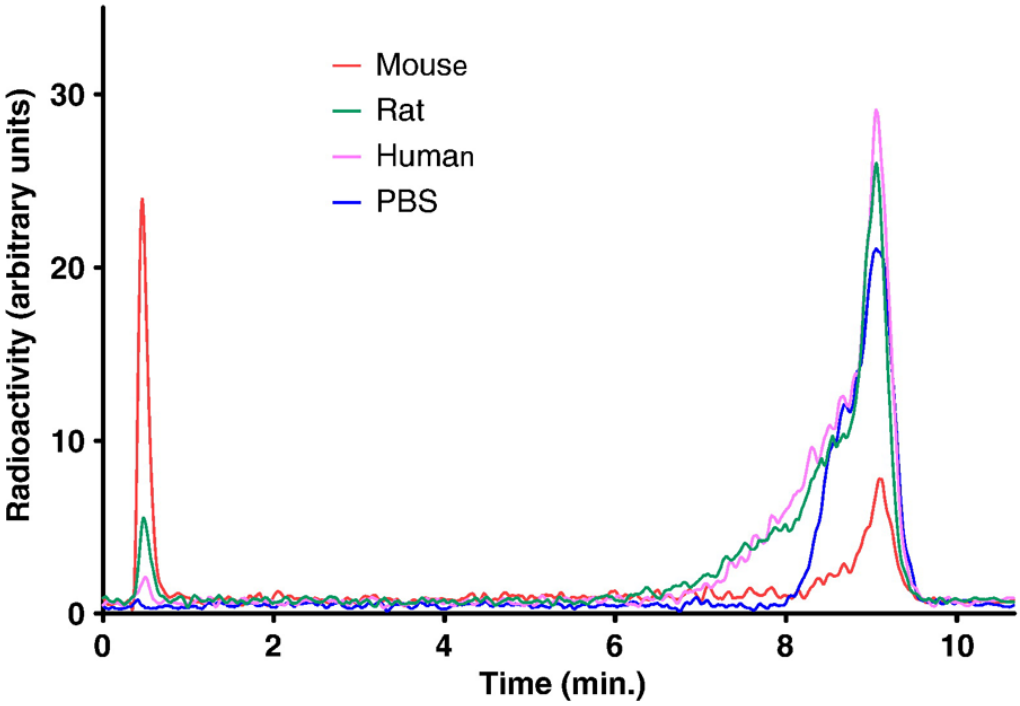

Figure 3.
Sample HPLC chromatograms of serum samples. Chromatograms were smoothed using the Savistsky-Golay method (20 neighbors, 2nd order)

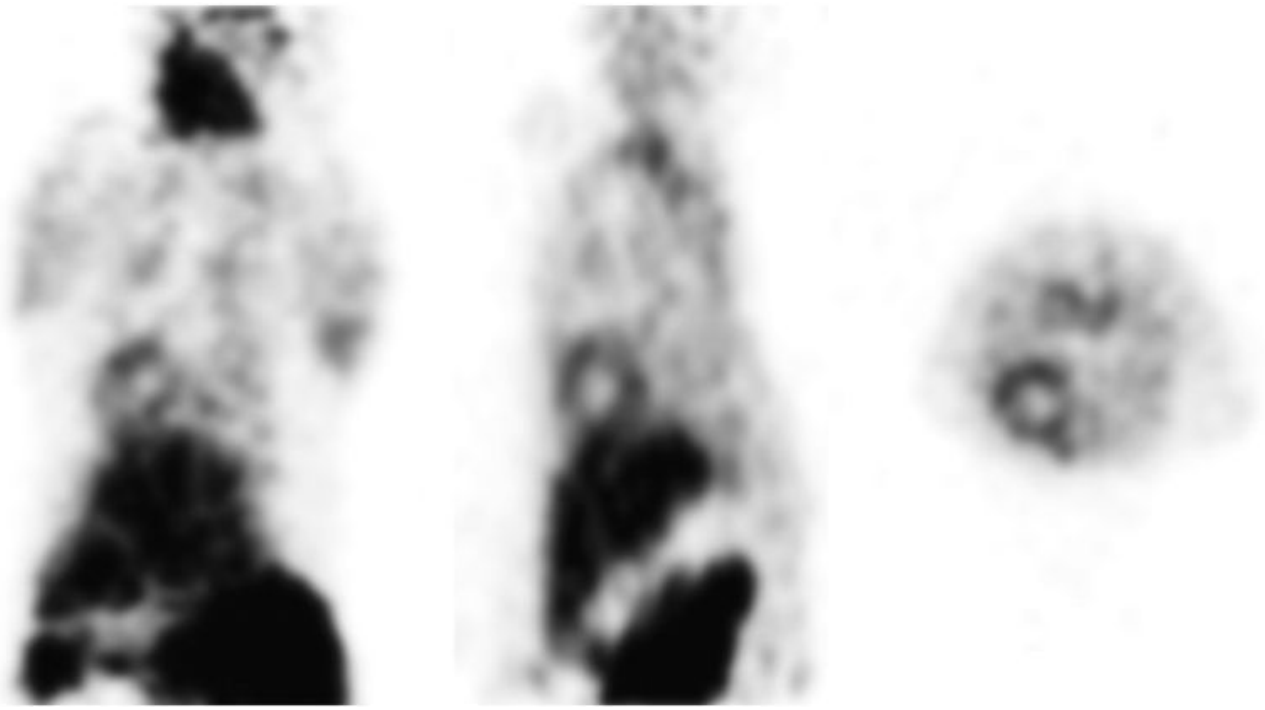

Figure 4.
MicroPET images of a rat injected with 2′-[^{18}F]fluoroethylrhodamine B.

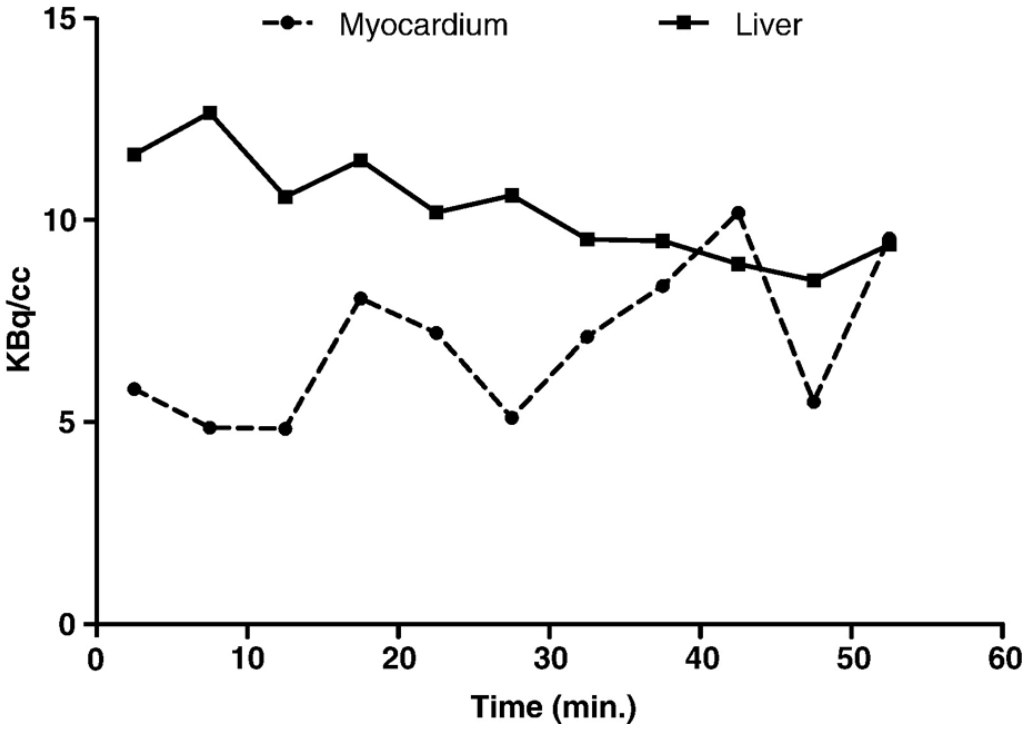

Figure 5.
Time activity curve of a rat myocardium and liver after injection with 2′-[^{18}F] fluoroethylrhodamine B

Table 1

Biodistribution of 2′-[^{18}F]fluoroethylrhodamine B in the rat. The results are presents as mean (ESD) % ID/gm at 1 h after the injection, n = 4.

Tissue	Mean (ESD)
Blood	0.08% (0.03%)
Lung	1.78% (0.65%)
Heart	2.06% (0.61%)
Liver	0.89% (0.07%)
Kidney	8.31% (0.81%)
Spleen	5.63% (0.78%)
Gut	2.40% (0.53%)
Muscle	0.16% (0.04%)
Skin	0.20% (0.02%)
Femur	0.45% (0.08%)